Available online at www.sciencedirect.com
SCIENCE DIRECT
Catalysis Today 107–108 (2005) 436–443
CATALYSIS TODAY
www.elsevier.com/locate/cattod

New Co-Ni catalyst systems used for methane dry reforming based on supported catalysts over an INT-MM1 mesoporous material and a perovskite-like oxide precursor $LaCo_{0.4}Ni_{0.6}O_3$

Orlando González [a,b,*], Juan Lujano [a], Eglé Pietri [b], Mireya R. Goldwasser [b]

[a] *PDVSA-INTEVEP S.A., Refining and Petrochemicals Division, 1070-A Caracas, Venezuela*
[b] *Centro de Catálisis, Petróleo y Petroquímica CCPP, Escuela de Química, Facultad de Ciencias, Universidad Central de Venezuela, Apartado 47102, Los Chaguaramos, Caracas, Venezuela*

Available online 22 August 2005

Abstract

To obtain a new, better-dispersed catalytic material on a stable substrate for the production of H_2 and CO by reforming of CH_4 with CO_2, a series of supported Ni-Co catalysts (designated C1, C2, C3 and C6) was prepared by impregnation of a mesoporous silica material (INT-MM1). Catalyst reactivity was compared with a $LaCo_{0.4}Ni_{0.6}O_3$ perovskite-like oxide synthesized by the citrate sol–gel method. All materials were characterized by several physico-chemical techniques: AA, EDX, XDR, IR, BET surface area and TPR. Significant differences in activity and product distribution were observed among the catalytic systems in the reforming reaction. The supported materials were active for the reaction, but selectivity for H_2 depended on the bimetallic composition of each solid. The different product distributions observed could be attributed to the properties of the support and their interaction with the metals. Among all of the solids investigated, C3 was the most selective toward the production of H_2, reaching values of 78%, and the perovskite-like oxide precursor was the most active solid, with conversion of 91%. Both catalyst systems have the same Co/Ni metal ratio (≅0.7) and were very stable for up to 100 h on stream.

Keywords: Dry reforming; Methane; Perovskite; Hydrogen; INT-MM1 silica

1. Introduction

Several oriented processes to obtain more valuable compounds from polluting low-cost gaseous streams with carbon-containing materials, such as methane and CO_2, by a dry reforming process have recently attracted considerable attention. The reforming of CH_4 with CO_2 has been intensively studied due to its important application in industry to produce synthesis gas [1,2]. This process offers certain advantages, such as a lower H_2/CO ratio, and seems to be more suitable for the Oxo and Fischer–Tropsch processes. From an environmental protection perspective, the use of harmful gases in this process would allow a decrease in global warming, through a decrease in the concentration of these greenhouse gases in the atmosphere.

This reforming process involves high temperatures and the presence of steam as a by-product from the reverse water-gas shift reaction (RWGS). Thus, sintering of the active metal species and coke formation can lead to catalyst deactivation and in some cases to plugging of the reactor. Therefore, it is necessary to design new catalyst formulations to overcome these problems. Reforming processes require active, selective and stable catalysts to resist the severe temperature conditions involved. Moreover, the catalysts should be economically accessible. Therefore, with the aim of obtaining highly dispersed catalyst systems for structure-sensitive reactions, such as the reforming of CH_4 with CO_2, this investigation proposed the use of Co-Ni supported systems impregnated over a mesoporous material, modifying the metal loading and comparing the results with a perovskite-like oxide precursor. Supported Ni catalysts have been used for this reaction, showing high activity comparable to noble metals [3,4]. The mesoporous material INT-MM1, a molecular sieve developed

* Corresponding author. Tel.: +58 212 330 79 97; fax: +58 212 330 77 23.
E-mail address: gonzalezont@pdvsa.com (O. González).

0920-5861/$ – see front matter © 2005 Elsevier B.V. All rights reserved.
doi:10.1016/j.cattod.2005.07.112

by PDVSA-INTEVEP [5], is an inert material based on silica. It has a high BET surface area and good thermal and hydrothermal stability. It presents tortuous channels of uniform diameter (≅25 Å) with short-range order and a high concentration of hydroxyl groups on its surface, which facilitates the incorporation of dispersed metal phases. This material has a bimodal pore distribution, with pore volume $V_p > 0.2$ ml/g. It is synthesized using conventional sol–gel methods. Among other applications, this material has been used as a selective adsorbent of polluting molecules in liquid streams, as a catalyst support in hydrocarbon selective oxidation, hydrotreatment reactions, fine chemistry and recently in dry reforming [6].

2. Experimental

2.1. Catalyst preparation

The supported catalysts C1 (24 wt.% Co), C2 (5 wt.% Co, 19 wt.% Ni), C3 (10 wt.% Co, 15 wt.% Ni) and C6 (24 wt.% Ni) were prepared by the incipient wetness method [7], simultaneously adding suitable amounts of an aqueous solution of the metal precursor to the mesoporous support, previously dried at 150 °C for 12 h. After impregnation, the support was dried at 70 °C for 12 h. Catalysts were calcined in air (30 ml/min) using the following protocol: from room temperature to 200 °C at a rate of 3 °C/min and left for 2 h, then heated to 450 °C at the same rate.

The INT-MM1 mesoporous material was supplied by PDVSA-INTEVEP. Its synthesis is reported elsewhere [5].

The perovskite-like precursor oxide $LaCo_{0.4}Ni_{0.6}O_3$ was synthesized by the sol–gel method, as previously reported [8,9]. The Co and Ni sources used in the preparation of these materials were hexahydrated nitrates of the respective metals (99.9%).

2.2. Characterization techniques

Chemical analysis of all samples was carried out using a Philips XI-30 scanning electron microscope coupled to an EDAX Dxi4 electron-dispersive X-ray device for quantitative analysis. Atomic absorption (AA) was used as a complementary technique for the analysis of some samples.

Specific areas were calculated by the BET method from nitrogen adsorption isotherms, recorded at liquid nitrogen temperature using a Micromeritics ASAP 2400 instrument, setting a value of 0.162 nm^2 for the cross-sectional area of the N_2 molecule adsorbed at −196 °C. Prior to adsorption measurements, samples were outgassed at 120 °C. The specific area of the samples ranged from 4 to 316 m^2/g.

Powder X-ray diffraction (XRD) patterns of the fresh, reduced and used samples were recorded using a Siemens D-8 advanced diffractometer with Cu $K\alpha_1$ ($\lambda = 1.54060$ Å) radiation for crystalline phase detection over the range of 2θ angles from 2° to 90°. The powder samples were reduced ex situ in H_2 (80 ml/min) at 700 °C for 3 h in a continuous flow system and then collected in isooctane before being transferred to the pretreatment chamber of the diffractometer. The metal crystallite size of the supported catalysts was calculated using the main reflection of the XRD patterns shown in Table 1 and the Scherrer formula corrected for instrumental line broadening.

A ThermoQuest TPD/R/O 110 instrument was used for temperature-programmed reduction (TPR) analyses. Reduction profiles were obtained by passing a 5 vol.% H_2/Ar flow at a rate of 20 ml/min through the sample (weight approximately 70 mg). The temperature was increased from 30 to 1000 °C at a rate of 10 °C/min.

2.3. Catalytic activity

Methane dry reforming was carried out using 200 mg of powder catalyst in a continuous-flow system provided with a fixed-bed quartz tubular reactor (20 mm i.d.) at atmospheric pressure. The reaction conditions were: CH_4/CO_2 feed molar ratio ≅ 1, using N_2 as diluent gas at $CH_4/CO_2/N_2 = 1:1:8$, GHSV = 24 l/(h g) and 700 °C, as previously described [8,9]. The reaction mixture was fed at a total flow rate of 80 ml/min using previously calibrated mixers and flow meters. The temperature of the catalytic bed and the furnace was monitored using nickel–nickel–chrome thermocouples.

Table 1
Chemical analysis and textural properties of supported catalyst systems

Catalyst materials	Metal loading		S_{BET}		D_{BJH} (Å)	$^*d_v$ (Å)
	Co content (wt.%)	Ni content (wt.%)	Fresh (m^2/g)	Used (m^2/g)		
Supported						
C1	24.0	0	304	168	32	34.5
C2	5.0	19.0	295	148	37	27.8
C3	10.0	15.5	316	193	35	28.8
C6	0	24.1	300	152	34	31.9
Perovskite						
$LaCo_{0.4}Ni_{0.6}O_3$	9.6	13.5	4	8	–	–
Support						
INT-MM1	–	–	1067	–	25	25

$^*d_v$, calculated from the main reflection (first diffraction peak) using Scherrer formula; D_{BJH}, pore diameter; S_{BET}, surface area.

Prior to catalytic tests, the catalysts were reduced in situ with a H_2 stream (80 ml/min) at 700 °C for 3 h. After reduction, the samples were flushed with N_2 for 15 min at the same temperature. Water produced during the reaction was condensed before passing the reactants and products through the analysis system, which consisted of an on-line gas chromatograph (Perkin-Elmer AutoSystem XL) equipped with a thermal conductivity detector and a Carbosieve SII 80/100 column (12′ × 1/8′ o.d.). Reactant conversion was defined as the amount of CH_4 and CO_2 converted per total amount of CH_4 and CO_2 fed, respectively.

Selectivity was defined as $SH_2\ (\%) = 2/4 \times nH_2(p)/[nCH_4(c)] \times 100$ for H_2 and SCO $(\%) = nCO(p)/[nCH_4(c) + nCO_2(c)] \times 100$ for CO, where $nH_2(p)$ and $nCO(p)$ represent the moles of product formed, and $nCH_4(c)$ and $nCO_2(c)$ the amount of methane and carbon dioxide converted.

3. Results and discussion

3.1. Morphological characteristics

The INT-MM1 support has a high BET specific surface area. Its adsorption–desorption isotherm does not present hysteresis, thus suggesting that channels in the material are formed by a uniform system of through-pores (open at both ends) that are interconnected. For this mesoporous material, the density function theory (DFT) method gave an average pore size (D_p) of 25 Å and a bimodal pore distribution was observed, with approximately 55% mesoporosity and 45% microporosity contributing to the total surface area of this material (>1000 m^2/g). Using thermogravimetric analysis, a composition of 58 wt.% SiO_2 was determined. Results for chemical analyses, the specific surface area for all catalyst systems before and after reaction, the pore diameter for fresh samples and the metal crystallite size for reduced samples tested under reaction conditions are shown in Table 1.

Surface area results for the fresh supported catalysts (Table 1) show an appreciable decrease in surface area compared to INT-MM1. This decrease is attributed to sintering of the support by thermal effects and mainly to complete obstruction of the microporous channels during impregnation of the metal precursors on this material. In addition, the textural properties of the calcined catalysts showed a mean pore distribution with diameters between 20 and 500 Å, another reason why the mesoporosity of the INT-MM1 support in these calcined samples is retained.

There was a decrease in surface area (≅40%) for the used catalysts compared to the fresh material according to the results shown in Table 1. This change in surface area can be attributed to sintering effects and carbon deposition on the metal crystallites, as indicated by the percentage carbon balance in Table 2. For the perovskite-like precursor the opposite effect was observed: the used material showed a higher surface area than the original precursor. It is possible that this increase in surface area is related to the formation of new material with other physical properties due to collapse of the original oxide under the reduction and reaction conditions.

Table 2
Catalytic properties of the catalyst systems tested in reaction

Catalysts	Supported catalyst systems				Precursor
	C1	C3	C2	C6	$LaCo_{0.4}Ni_{0.6}O_3$
CH_4 conversion (%)	71	72	92	95	91
CO_2 conversion (%)	80	74	98	98	99
CH_4/CO_2 feed ratio	1.09	0.77	0.64	0.77	0.80
Selectivity to H_2 (%)	27	78	39	33	27
Selectivity to CO (%)	65	85	71	70	89
Carbon balance (%)	35	15	29	30	11
H_2/CO ratio	0.42	0.92	0.55	0.47	0.30
Co/Ni metal ratio	–	0.64	0.26	–	0.71

W = 200 mg, GHSV = 24 L/(h g), time on stream = 24 h, atmospheric pressure, T = 700 °C and gas mixture composition: $CH_4/CO_2/N_2$ = 1:1:8.

3.2. X-ray diffraction and infrared analysis

XRD and IR spectra of the $LaCo_{0.4}Ni_{0.6}O_3$ precursor were recorded to confirm the presence of the expected perovskite-like oxide. These analyses prove that the sol–gel method produces solids with high crystallinity, homogeneity and purity. According to Fig. 1, the IR spectra of this material showed two broad bands characteristic of the perovskite-like structure: ν_1 localized between 600 and 650 cm^{-1} and ν_2 at 400–420 cm^{-1}. The first band ν_1 is attributed to the stretching vibration and the second one ν_2 to the deformation produced by changes in the bond angles between oxygen atoms of the perovskite-like structure.

Fig. 2a shows the XRD pattern for fresh $LaCo_{0.4}Ni_{0.6}O_3$, with a typical ABO_3 structure as the main phase. XRD spectra of this sample after the reduction procedure showed the presence of metallic phases of Co and Ni, including a matrix of La_2O_3 (Fig. 2b). Comparison of XRD patterns for this material shows that the precursor is able to generate a catalyst in situ, in which the metal species that thermally evolve from the perovskite lattice via metal migration are spontaneously deposited on a La_2O_3 matrix, formed during the reaction as a consequence of collapse of the original structure. When a perovskite-like oxide is used as a catalyst precursor, after in situ H_2 pretreatment, well-dispersed metallic particles on a La_2O_3 matrix are formed. It has been reported that the metallic crystallite size for this type of catalyst precursor is of nanometer dimensions, associated with a high degree of metal dispersion [4].

Fig. 3 shows XRD patterns for the supported catalyst systems on the mesoporous material, including the typical XRD pattern for the INT-MM1 used as the catalyst support in this reaction. Fig. 3a shows the XRD pattern of the INT-MM1 support, which consists of two characteristic peaks. One peak is located in the low-angle region and reflects short-range order related to the spatial organization of

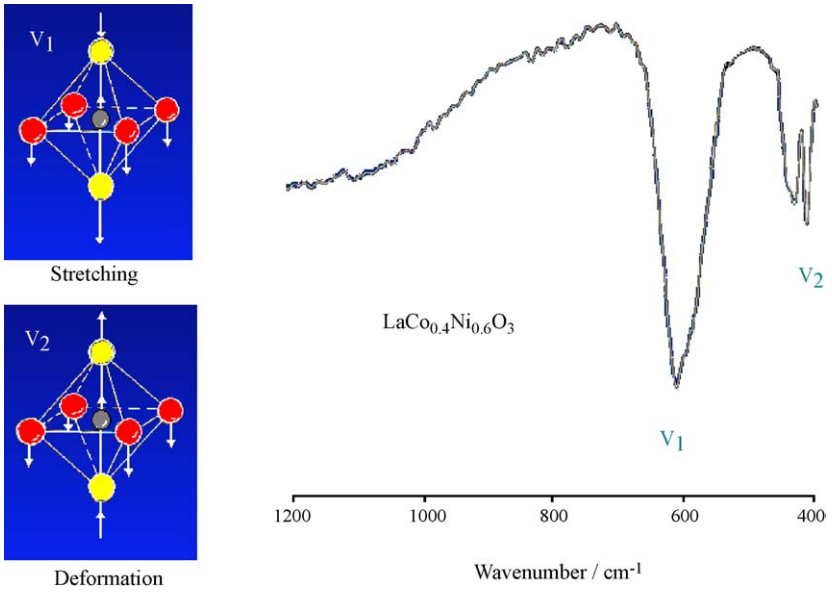

Fig. 1. Infrared spectra of the perovskite-like oxide precursor.

channels in the material. The second peak is located at 23° (2θ scale) and is attributed to diffuse dispersion caused by the lack of long-range order of Si atoms located on the walls of the channels in the material.

XRD analysis of the reduced catalysts on INT-MM1 as shown in Fig. 3b–e indicates that signals corresponding to the mesoporous support do not interfere with the diffraction signals of the metallic species. All the XRD patterns of the supported systems clearly reveal phases belonging to Co^0 and Ni^0, including signals attributed to the INT-MM1 material.

XRD analysis allowed qualitative measurement of the metal crystallite size in each catalyst system, based on estimations calculated using the Scherrer formula. Table 1 shows that the metal crystallite size values of the supported samples were similar.

Although the total amount of metal and the metal particle size were similar in all the catalysts prepared, we believe that the relative intensities of the XRD patterns for the supported catalysts depend on the nature of the metal oxide precursor phases formed during the calcination step. These metal oxide precursor phases can have an appreciable metal

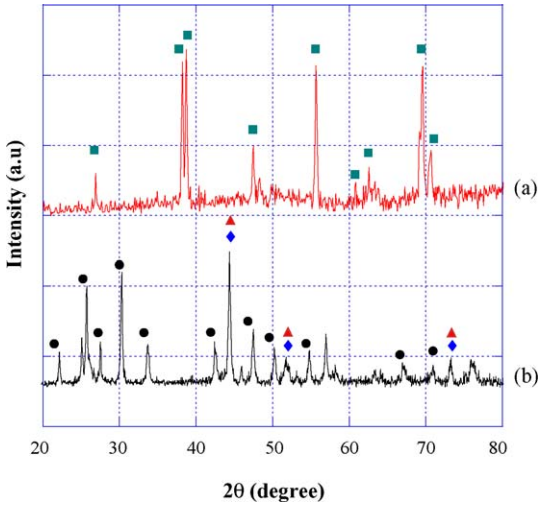

Fig. 2. XRD patterns of the perovskite-like oxide $LaCo_{0.4}Ni_{0.6}O_3$: (a) fresh sample and (b) reduced sample. Phases: (■) $LaCo_{0.4}Ni_{0.6}O_3$, (●) La_2O_3, (◆) Ni^0 and (▲) Co^0.

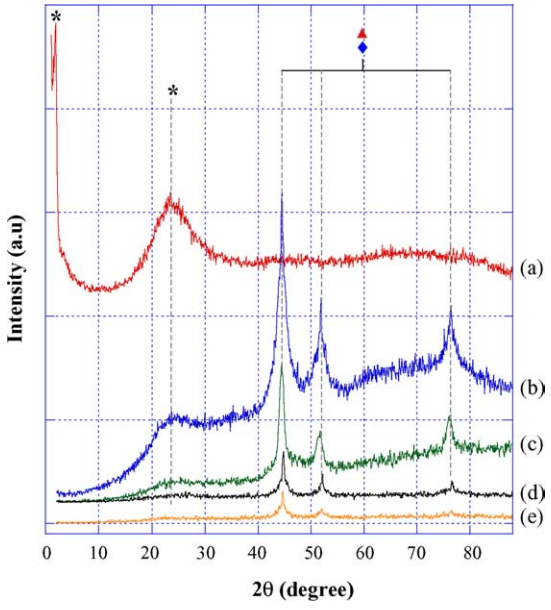

Fig. 3. XRD patterns of the supported catalyst systems over INT-MM1: (a) INT-MM1 support, (b) C3 reduced sample, (c) C1 [24 wt.% Co] reduced sample, (d) C6 [24 wt.% Ni] reduced sample and (e) C2 reduced sample. Phases: (*) INT-MM1 support, (◆) Ni^0 and (▲) Co^0.

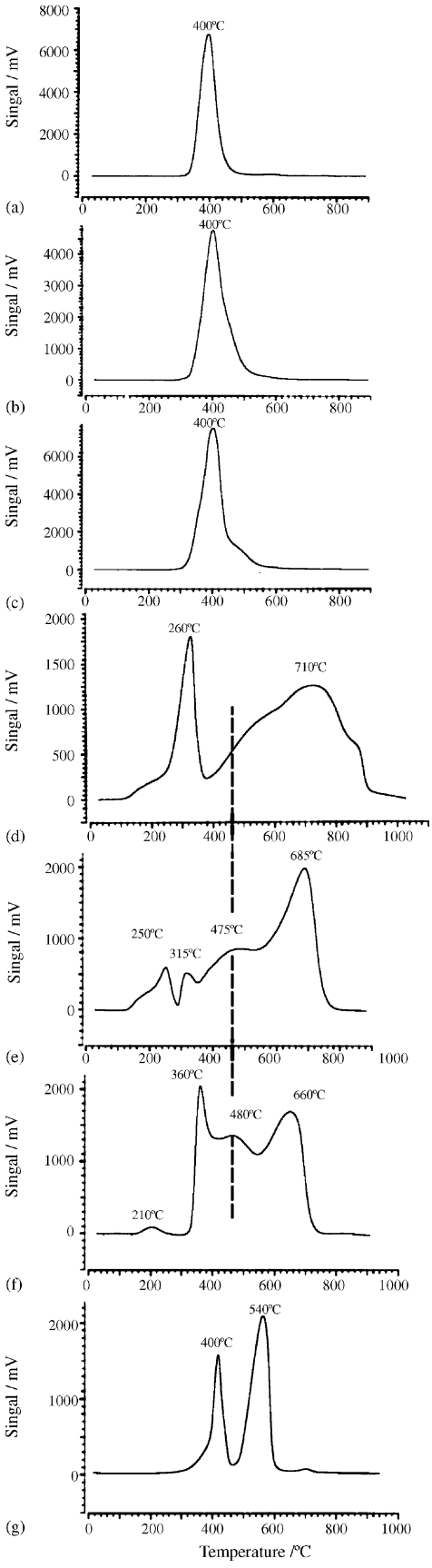

Fig. 4. TPR profiles of the calcined catalytic samples. (a) CoO (b) NiO (c) physical mixture of CoO and NiO, (d) C1 [24 wt.% Co] catalyst, (e) C3 catalyst, (f) C6 [24 wt.% Ni] catalyst and (g) $LaCo_{0.4}Ni_{0.6}O_3$.

content and different degrees of reducibility, depending on their stability, as shown by the TPR profiles (Fig. 4). It is believed that the reduced samples with lower intensities consist of very stable nanoparticles of metal oxides that are very difficult to reduce (e.g. Ni nanophases or Co spinels).

3.3. Temperature-programmed reduction

Fig. 4 shows TPR profiles for all the catalysts, including samples of commercial CoO and NiO used as references, and a profile for a physical mixture of these oxides. The profiles for the commercial CoO (Fig. 4a) and NiO (Fig. 4b) show only a reduction peak at approximately 400 °C, attributed to the reduction of Co^{2+} and Ni^{2+} to $Co^0$and Ni^0. Fig. 4c shows the TPR profile for the physical mixture of these metal oxides; a slight shift to higher temperature is observed in comparison to the single oxides. This behavior can be attributed to a weak metal–metal interaction during the reduction process.

Metal–metal interactions can take place during the reduction process for all the prepared bimetallic catalysts prepared, since the metal loading and temperature conditions used in the preparation and testing of these materials favor Co–Ni alloy formation according to the alloy phase diagrams established for these bimetallic systems [10].

The TPR profile for C1 (24 wt.% Co) shown in Fig. 4d has two reduction peaks localized at 260 and 710 °C, which are shifted to higher temperature in comparison to the profile for the physical mixture. This can be attributed to a strong metal–support interaction that leads to difficulties in completely reducing the Co active phase.

On the other hand, samples with metal loading based on Ni, such as C3 (Fig. 4e) and C2 (Fig. 4f) showed four reduction peaks, at 200–250, 315–360, 440–480 and 665–685 °C. The TPR profiles for the bimetallic catalysts have a very similar shape to the TPR profile for C6 (24 wt.% Ni) since they show a signal in common that is not evident in the profile of C1 (24 wt.% Co). This signal or reduction peak located in the temperature interval 440–480 °C could be attributed to Ni active species responsible for the catalytic behavior experimentally observed for each of these materials. In general, the presence of reduction peaks above 400 °C for all solids allow inference of the possibility that metal–support interactions hinder the reduction of several metal oxide precursor phases formed during the calcination of these materials.

With stronger metal–support interactions, the reduction peaks shift to higher temperatures. Based on the peak positions, reduction of C1 can be considered difficult, since its TPR profile presented a reduction peak localized above 700 °C. The catalytic behavior of this sample can be accounted for by a metal–support interaction effect, whereby a good portion of small metallic particles interacts

strongly with the support in the form of stable metal oxides. This small portion of particles could be in the form of very stable Co oxide species produced in the calcination step, such as Co spinel-like oxides, which are stable and difficult to reduce and to detect by XRD analysis.

Two reduction peaks at 400 and 540 °C were observed for the perovskite-like oxide precursor (Fig. 4g). These peaks are due to a two-step reduction of the perovskite structure $LaCo_{0.4}Ni_{0.6}O_3$, corresponding to the reduction of Co^{3+} and Ni^{3+} to Co^{2+} and Ni^{2+} (first step) and the reduction of these last species to Co^0 and Ni^0, respectively (second step). The reduction temperatures achieved for this precursor reveal a possible Co–Ni metal interaction, since these temperatures are between the temperatures recorded in previous work for $LaCoO_3$ and $LaNiO_3$ precursors [8]. The perovskite-like oxides based on Ni are non-stoichiometric compounds, able to stabilize Ni^{2+} and Ni^+ particles, which account for incomplete reduction and some difficulty in accurately determining hydrogen consumption [11]. The La_2O_3 matrix observed is produced as a consequence of the collapse of the original structure. It is a non-porous crystalline oxide with low surface area. The metal–support interactions observed for this precursor could be considered moderate, since it presented easily reducible and very active species in comparison to other supported catalysts.

The reducibility order based on the ease of reduction of these materials was as follows: $LaCo_{0.4}Ni_{0.6}O_3 > C3 > C6 > C1$. According to this, it is evident that the bimetallic systems (C2 and C3) have a high degree of reducibility compared to the monometallic systems. This could be attributed to an activated reduction process, in which the first metallic species reduced is able to accelerate reduction of the second metallic species due to the production of atomic hydrogen ($H^\bullet$) in the environment.

For C3 and the perovskite-like oxide, both with the same bimetallic loading, the nature of the support imposes a particular chemical environment. This means that samples with the same loading of bimetallic oxides can experience different levels of difficulty in reduction, allowing the formation of the metal species or active sites necessary for the reaction through nucleation mechanisms.

3.4. Catalytic activity

Table 2 shows the catalytic properties of the supported catalysts and the perovskite-like oxide precursor tested for the CO_2 reforming of methane. This table compares values for the CH_4 and CO_2 conversion, H_2 and CO selectivity, carbon balance, Co/Ni metal ratio, CH_4/CO_2 experimental feed ratio, and H_2/CO experimental product ratio. Under the used experimental conditions, all the catalyst systems were active for the studied reaction, with reactant conversion above 71%. Similarly, steady-state conditions for these systems were rapidly reached, remaining almost constant for up to 24 h on stream. Almost all the solids tested in this reaction showed high selectivity for CO, with values above 65%, and low selectivity for H_2, with values between 27 and 39%, except for C3 with a Co/Ni metal ratio ≅0.7, which showed selectivity of 78%. Thus, C3 showed the highest selectivity for the hydrogen production.

On the other hand, methane conversion values were slightly lower than those for carbon dioxide in all samples tested except for C3, for which the reactant conversions were similar. This indicates that for C1, C2, C6 and $LaCo_{0.4}Ni_{0.6}O_3$, other reactions take place simultaneously with the reforming reaction (1), such as the RWGS reaction (2) and the Boudouard reaction (4), according to the following reactions:

$$CH_4 + CO_2 \leftrightarrow 2CO + 2H_2,\ \Delta H_{298} = 247\,\text{kJ/mol} \quad (1)$$

$$CO_2 + H_2 \leftrightarrow CO + H_2O,\ \Delta H_{298} = 41.2\,\text{kJ/mol} \quad (2)$$

$$CH_4 + 2CO_2 \leftrightarrow 3CO + H_2O,\ \Delta H_{298} = 288.2\,\text{kJ/mol} \quad (3)$$

$$2CO \leftrightarrow C + CO_2,\ \Delta H_{298} = -172\,\text{kJ/mol} \quad (4)$$

Reaction (3) results from a combination of the dry reformation and RWGS reactions. Taking into account that the CH_4/CO_2 experimental feed ratios for solids C1, C2, C6 and $LaCo_{0.4}Ni_{0.6}O_3$ varied between 0.64 and 1.09 (Table 2), reaction (3), with a CH_4/CO_2 stoichiometric ratio of 1/2, could explain the differences obtained in product distribution, which are almost in agreement with the H_2/CO stoichiometric ratio 1/3, also listed in Table 2 for these solids. According to these observations, it is clearly possible that the catalytic behavior of the supported catalyst systems on INT-MM1 depends on both the Co/Ni metal ratio and type of metal–support interaction that can take place in each case. The product distribution differences obtained for these supported solids can be attributed to the interaction level produced between the used Co–Ni metal loading and the INT-MM1 support. This same bimetal loading ratio could be related to the metal particle size produced in each system during H_2 pretreatment of fresh samples, and could also influence metal dispersion, which plays a fundamental role in this type of structure-sensitive reaction [12]. For these supported catalyst systems on INT-MM1, the formation of very stable metal oxide species that are difficult to reduce cannot be discounted, for example, the formation of Ni nanophases or Co spinels that can not be detected by XRD analysis. Similarly, the probability for the formation of Co–Ni alloys [10] and of small size particles that are able to interact strongly with the support, are worth arguments to considering in this work.

It is possible that for C3 an equilibrium was established between the bimetal loading ratio and the mesoporous support that allowed retention and better dispersion of the active phases over the mesoporous surface. In this case, the porous structure of the INT-MM1 material through its channels could act as a spreading agent, which prevents metal sintering caused by increased temperature and leads to

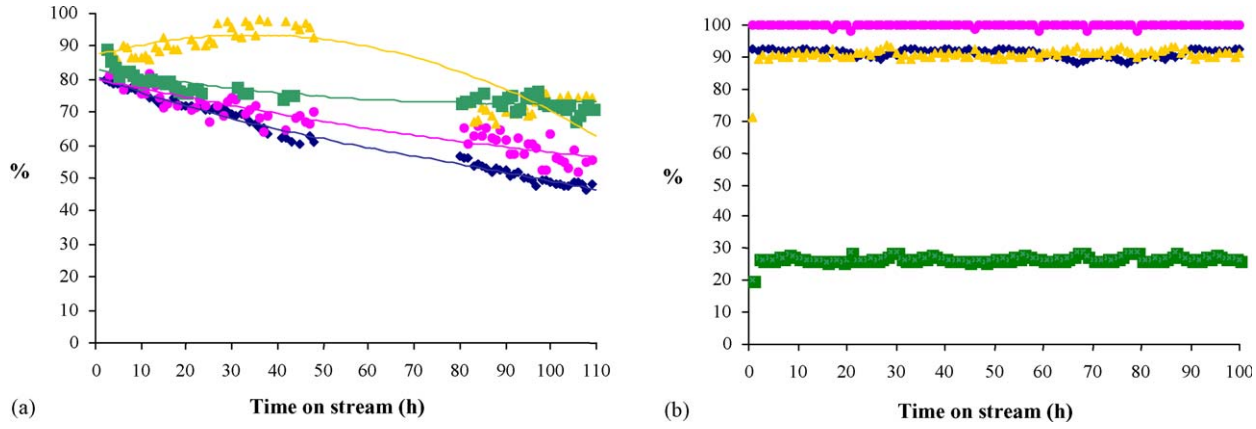

Fig. 5. Catalytic properties vs. time on stream. (a) C3 solid and (b) perovskite-like oxide, (◆) CH_4 conversion (%), (●) CO_2 conversion (%), (■) selectivity to H_2 (%) and (▲) selectivity to CO (%). W = 200 mg, GHSV = 24 L/(h g), CH_4/CO_2 feed ratio ≅ 1, atmospheric pressure, T = 700 °C, gas mixture composition: $CH_4/CO_2/N_2$ = 1:1:8.

a particular metal–support interaction produced only under these conditions.

For C3 and the perovskite-like precursor, which had the same metal loading (Co/Ni ≅ 0.7) but dispersed on different supports, the great difference in H_2 selectivity is very interesting (Table 2; Fig. 5). In these catalysts, the product distribution was also strongly influenced by the support. For the perovskite-like precursor oxide, the La_2O_3 matrix produced as a consequence of collapse of the original structure does not have a high specific surface area (2 m^2/g) suitable for dispersion of the active phases; moreover, this support is a crystalline oxide without porous structure. Thus, it is possible that metal sintering can take place in this precursor system, inducing parallel reaction to decrease the H_2 selectivity. Tests of the catalytic stability of C3 (Fig. 5a) and the perovskite-like oxide precursor (Fig. 5b) showed an approximate loss of 25% in initial reactant conversion for C3 due to carbon deposition on the metal crystallites, as indicated by the percentage carbon balance in Table 2. However, after 110 h on stream its H_2 selectivity remained almost constant. The perovskite-like oxide precursor showed a marked difference in product distribution, which remained constant during all the time on stream (Fig. 5b). Of all the catalysts, the C3 supported material was the most selective for the production of H_2, reaching values of 78%, and the perovskite-like oxide precursor was the most active solid, reaching conversion of 91%. Both catalyst systems have the same Co/Ni metal ratio and were very stable for up to 100 h on stream.

4. Conclusions

The different characterization techniques used revealed the in situ production of well-dispersed metallic particles using perovskite-like oxides as precursors. Well-dispersed Co–Ni metallic particles were produced on the La_2O_3 matrix as a consequence of the collapse of the original structure of $LaCo_{0.4}Ni_{0.6}O_3$ after reduction. This collapsed precursor system showed high activity for methane dry reforming, with conversion values for CH_4 and CO_2 of 91 and 99%, respectively, and low H_2 selectivity. The catalytic performance of the supported systems on the mesoporous material strongly depended on the Co–Ni loading or metal ratio present in the catalyst support. This metal ratio impregnated in an INT-MM1 support significantly influences the product distribution obtained. The C3 catalyst with a Co/Ni metal ratio of 0.7 was the most selective solid for the production of H_2, reaching values of 78%, higher to those for the other catalysts prepared. It is possible that the porous structure of the INT-MM1 mesoporous material could prevent metal sintering of the metallic phases due to the order of its channels and to the metal–support interactions that could take place for the C3 bimetallic ratio in particular.

Acknowledgments

The authors acknowledge Universidad Central de Venezuela through CCPP, the C1 Chemistry Group and PDVSA-INTEVEP, S.A. for their support of this research.

References

[1] J.R. Rostrup-Nielsen, Stud. Surf. Sci. Catal. 81 (1993) 25.
[2] M.C.J. Bradford, M.A. Vannice, Catal. Rev. Sci. Eng. 41 (1999) 1.
[3] S.M. Stagg-Williams, F.B. Noronha, G. Fendley, D.E. Resasco, J. Catal. 194 (2000) 240.
[4] J.R. Rostrup-Nielsen, J.H. Bak Hansen, J. Catal. 144 (1993) 38.
[5] J. Carraza, J. R. Córdova, J. Lujano, J. M. Cruz, US Patent 5,840,271, November 24, 1998.
[6] O. González, J. Lujano, H. Molero, M. Pacheco, E. Pietri, M.R. Goldwasser, in: Proceedings of the 18th North American Catalysis Society Meeting, Cancún- México, June 1–6, 2003, p. 322.
[7] G. Leofanti, M. Padovan, G. Tozzola, B. Venturelli, Catal. Today 41 (1998) 207.

[8] M.R. Goldwasser, M.E. Rivas, E. Pietri, M.J. Pérez-Zurita, M.L. Cubeiro, L. Gingembre, L. Leclercq, G. Leclercq, Appl. Catal. 225 (2003) 45.
[9] E. Pietri, A. Barrios, O. González, M.R. Goldwasser, M.J. Pérez-Zurita, M.L. Cubeiro, J. Goldwasser, L. Leclercq, G. Leclercq, L. Gingembre, Stud. Surf. Sci. Catal. 136 (2001) 381.
[10] ASM Handbook of Material Engineering, vol. 3, Phase Diagrams, Hardbound; ASM Publication, 1992, ISBN 0-87170-381-5.
[11] J. Barbero, M.A. Peña, J.M. Campos-Martin, J.L.G. Fierro, P.L. Arias, Catal. Lett. 81 (2003) 211.
[12] G.J. Kim, D. Cho, K. Kim, J. Kim, Catal. Lett. 28 (1994) 41.